

RD-A172 006

HOLE GRATINGS AND DIFFRACTION OF GAUSSIAN BEAMS(U)  
PENNSYLVANIA STATE UNIV UNIVERSITY PARK DEPT OF PHYSICS  
T A WIGGINS 15 MAR 86 AFOSR-TR-86-0641 AFOSR-83-0258

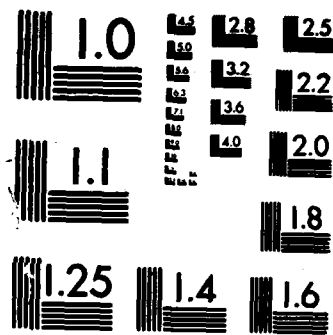
1/1

UNCLASSIFIED

F/G 20/6

NL

##  
[REDACTED]  
[REDACTED]



MICROCOPY RESOLUTION TEST CHART  
NATIONAL BUREAU OF STANDARDS-1963-A

2

Unclassified  
SECURITY CLASSIFICATION OF THIS PAGE (When Data Entered)

REPORT DOCUMENTATION PAGE		READ INSTRUCTIONS BEFORE COMPLETING FORM
1. REPORT NUMBER <b>AFOSR-TR. 86-0641</b>	2. GOVT ACCESSION NO.	3. RECIPIENT'S CATALOG NUMBER
4. TITLE (and Subtitle)  Hole Gratings and Diffraction of Gaussian Beams		5. TYPE OF REPORT & PERIOD COVERED Final, 7/1/83-12/31/84
		6. PERFORMING ORG. REPORT NUMBER
7. AUTHOR(s)  T. A. Wiggins, Professor of Physics		8. CONTRACT OR GRANT NUMBER(s)  AFOSR-83-0258
PERFORMING ORGANIZATION NAME AND ADDRESS Department of Physics The Pennsylvania State University 104 Davey Lab University Park, PA 16802		10. PROGRAM ELEMENT, PROJECT, TASK AREA & WORK UNIT NUMBERS 6/102F 2306 D9
11. CONTROLLING OFFICE NAME AND ADDRESS AFOSR/PKD Bldg. 410 Bolling AFB, DC 20332		12. REPORT DATE March 15, 1986
		13. NUMBER OF PAGES 2 + reprint
14. MONITORING AGENCY NAME & ADDRESS (if different from Controlling Office) AFOSR/NE Bldg. 410 Bolling AFB, DC 20332  NE		15. SECURITY CLASS. (of this report)  Unclassified
		15a. DECLASSIFICATION/DOWNGRADING SCHEDULE
16. DISTRIBUTION STATEMENT (of this Report)  Approved for public release; distribution unlimited		
17. DISTRIBUTION STATEMENT (of the abstract entered in Block 20, if different from Report)  DTIC ELECTE SEP 17 1986 S B D		
18. SUPPLEMENTARY NOTES		
19. KEY WORDS (Continue on reverse side if necessary and identify by block number)  Gaussian beams, hole gratings, diffraction		
20. ABSTRACT (Continue on reverse side if necessary and identify by block number) Methods for the determination of waist size and position for Gaussian beams are summarized and an alternative method which applies to pulse systems was proposed and tested. The general theory of Fraunhofer diffraction of Gaussian beams was developed which permitted a new method for location of laser waists. An extension to Fresnel diffraction was proposed. The use of hole gratings for production of multiple spots for damage threshold measurements is inherent to this work. The effects of their characteristics on the intensity profile are included.		

AD-A172 006

DTIC FILE COPY

**AFOSR-TR. 86-0641**

AIR FORCE OFFICE OF SCIENTIFIC RESEARCH (AFSC)  
OFFICE OF TRANSMITTAL TO DTIC  
This technical report has been reviewed and is  
approved for public release IAW AFR 190-12.  
Distribution is unlimited.  
MATTHEW J. KERPER  
Chief, Technical Information Division

**Hole Gratings and Diffraction of Gaussian Beams**

**Final Report**

**March 15, 1986**

**Approved for public release;  
distribution unlimited.**

**Contract AFOSR-83-0258  
July 1, 1983-December 31, 1984**

**T. A. Wiggins, Principal Investigator  
The Pennsylvania State University  
Department of Physics  
University Park, PA 16802**

**Approved for public release; distribution unlimited**

**86 9 15 09**

## FINAL REPORT

This is the final report on Contract AFOSR-83-0258, entitled "LASER DAMAGE THRESHOLDS IN PLASTICS." The original termination date of July 1, 1984 was extended to December 31, 1984.

The objectives of the work were to: determine damage thresholds for plastics at 694 nm; and continue the optimization of the use of hole gratings for producing multiple damage spots for a study of small-scale damage.

## ACCOMPLISHMENTS

### Damage Thresholds

The original intent was to determine laser damage thresholds on plastics produced in a clean environment at the Seiler Laboratory, U.S. Air Force Academy, at the ruby wavelength (694 nm) as a supplement to studies at the Seiler Laboratory at 1060 nm. No results were obtained since no plastics of sufficiently high quality to warrant testing were produced during the duration of the contract.

### Methods for Determination of Waist Size

The original work on the use of hole gratings for laser damage testing which was published in Applied Optics 22, 3388 (1983) indicated that while trial and error methods of determining optimum focusing conditions were available, a systematic method would be useful for the prediction of the position and size of the best focus for pulsed systems. This prediction is dependent upon a knowledge of the characteristics of the laser system including the size and position of its waist. A method for determining these quantities was proposed and tested using both a cw laser for exploratory investigation, and a pulsed ruby system as an example. The proposed method involves the measurement of beam size at two different distances from the back focal point of a lens.

These can be measured simultaneously for a single pulse using a beam splitter. The results indicated that the waist size could be determined with an error of about 5% and that its position could be determined within 10% of the Rayleigh length of the laser's output beam. These data would then allow a prediction of the position and size of the best focus for damage threshold measurements.

#### Hole Gratings

The use of hole gratings for producing multiple spots useful in damage testing was discussed in the publication noted above. This work was extended to a general treatment of Fraunhofer diffraction of Gaussian beams.

The result of this study was the prediction and experimental verification of interference details in the region between the intense multiple spots which permits an alternative method for the location of the waist of a laser system. The extension of this work to the case of Fresnel diffraction was also suggested and is currently under investigation.

The work noted above was published in Applied Optics 24, 1350 (1985), a reprint of which is attached.

#### PERSONNEL

The Principal Investigator was T. A. Wiggins, Professor of Physics. He was assisted by John Pardo, a graduate student in Physics. He now is at Eastman Kodak, Rochester, NY. His Master's paper entitled "A New Technique for the Characterization of a Spherical Gaussian Laser Beam" was a part of the publication noted above. His degree was awarded in December 1984. Also contributing to the work was R. M. Herman, Professor of Physics.



DTIC TAB	
Unannounced	
Justification	
PER CALL M	
By	
Distribution/	
Availability Code	
Dist	Availability Code/ or Special
A-1	

# Diffraction and focusing of Gaussian beams

R. M. Herman, John Pardo, and T. A. Wiggins

Methods for the measurement of the waist size and position for Gaussian beams are summarized. An alternative method is given which would apply to pulsed systems. The general theory of diffraction of Gaussian beams is developed which provides a new method for the location of the beam waist. These methods which use hole gratings are employed to demonstrate their feasibility using a small cw source.

## I. Introduction

The propagation and focusing of Gaussian beams was first discussed by Fox and Li<sup>1</sup> who showed that only two parameters are required to predict the beam characteristics at any distance from its source. This work has been summarized and discussed by Kogelnik and Li<sup>2</sup> and by Siegman.<sup>3</sup> More recently, work by Li and Wolf,<sup>4</sup> Carter,<sup>5</sup> Self,<sup>6</sup> Luxon *et al.*,<sup>7</sup> and Anderson<sup>8</sup> has extended the theory and discussed the structure of a focused beam.

The parameters usually chosen are those of the size of waist  $w_0$ , the smallest radius of the beam for which the intensity is  $1/e^2$  of the on-axis value, and the position of the waist. Alternatively, the Rayleigh length  $z_R$  can be used where  $z_R = \pi w_0^2/\lambda$ . This length corresponds to a distance of propagation to a point where the  $1/e^2$  radius of the beam is  $\sqrt{2}$  times that at the waist, or the on-axis intensity is one-half of that at the waist. The Rayleigh length can thus be considered to be the half-intensity width of the Lorentzian on-axis intensity distribution along the beam.<sup>6</sup>

For applications such as coupling of Gaussian beams into spherical interferometers and optical waveguides, or for predicting the position and size of the image waist formed by a lens, these parameters must be known or measured. In laser damage studies it is especially important to know these quantities to determine thresholds. Although it is desirable to make a direct measurement of the beam size at the damage site, knowledge of these quantities will assist in the selection of the focal length and the distance from the laser to the lens to be

used, especially for spot-size effect investigations. Also, in a study of volume damage, it may not be feasible to make a direct measurement.

A particularly useful formulation has been given by Self.<sup>6</sup> In addition to statements concerning the size of a propagating beam and the radius of curvature of the wave front, he has presented equations for the position and size of the waist formed by a lens and for the new Rayleigh length. The equation for the position is analogous to the thin lens equation used for classical optics and is shown to reduce to this for  $z_R = 0$ .

It is the purpose of this writing to summarize methods which have been reported for the measurement of the beam parameters, to present a modification of Self's equations, and to describe a new interferometric method for the determination of the position of the beam waist from measurements made at the focal point of a lens. This is based on a general theory of diffraction of Gaussian beams which is presented here. Some experimental results for a He-Ne laser are included.

## II. Modification of Self's Equations

The equation given by Self<sup>6</sup> for the position  $s'$  of the image waist formed by a lens of focal length  $f$  when an object waist of size  $w_0$  is placed a distance  $s$  from the lens is

$$(s'/f) - 1 = \frac{(s/f) - 1}{(s/f - 1)^2 + (z_R/f)^2}.$$

The size of the image waist  $w'_0$  is calculated from  $w'_0 = mw_0$  using the magnification which Self gives as  $m = 1/[(s/f - 1)^2 + (z_R/f)^2]^{1/2}$ , the Rayleigh length of the output beam being  $z'_R = m^2 z_R$ . It is noted that by reversing the direction of the beam, the position and size of the input waist can be computed from the output waist size and position using  $z_R = \pi w_0^2/\lambda$ .

The presence of the quantities  $(s/f - 1)$  and  $(s'/f - 1)$  suggests that the equations can be reformulated in a form analogous to the Newtonian form of the lens equation for classical optics. Using the symbols  $x$  and  $x'$  to denote the distances of the object and the image

When this work was done all authors were with Pennsylvania State University, Physics Department, University Park, Pennsylvania 16802; J. Pardo is now with Eastman Kodak Company, Rochester, New York 14650.

Received 24 December 1984.

0003-6935/85/091346-09\$02.00/0.

© 1985 Optical Society of America.

from their respective focal points, it can be shown that  $xx' = f^2$ , and the lateral magnification is  $m = x'/f = f/x' = \sqrt{x'/x}$ . The longitudinal magnification is then  $m^2$ . In an analogous manner, defining  $y = s - f$  and  $y' = s' - f$ , Self's equations take the form

$$y' = \frac{yf^2}{y^2 + z_R^2} \quad \text{and} \quad m = \sqrt{y'/y} = \frac{f}{\sqrt{y^2 + z_R^2}}.$$

Since the waist positions here are measured from the front and back focal points whose positions can be precisely located by autocollimation, no determination of the position of the nodal planes of the lens is required as would be the case using the quantities  $s$  and  $s'$ . Clearly these equations reduce to the Newtonian equations for  $z_R = 0$ . One difference should be noted. While the new Rayleigh length  $z'_R = m^2 z_R = z_R \cdot y'/y$ , the longitudinal magnification is given by  $dy'/dy = m^2(z_R^2 - y^2)/(z_R^2 + y^2)$ . These equations give the same results as those of Self but have been found useful for their simplicity in calculations and measurement.

It is important to recognize that the maximum intensity in a focused beam does not necessarily occur at the focal point of a lens. As noted by Self<sup>6</sup> and Carter,<sup>5</sup> the maximum intensity can occur inside or outside the focal point, being at the focus only for the case of  $s = f$  or  $y = 0$ , for which condition the magnification is  $f/z_R$ .

### III. Determination of Waist Size and Position

The traditional method for determining the waist size  $w_0$  of the beam from a laser system has been from a measurement of beam divergence. If the  $1/e^2$  radius of a beam  $w$  can be measured at a large distance  $z$  from the source,  $w_0 = \lambda z/\pi w$ , where  $\lambda$  is the wavelength. The limitations to this method are that  $z$  is measured from the waist whose position may not be known and that an estimate of  $w_0$  or  $z_R$  must be at hand before the measurement since large  $z$  implies that measurements are made in the far field, that is, several times  $z_R$ . A less direct method but with fewer limitations is the measurement of the beam size  $w_f$  at the focus of a lens or mirror. Here  $w_0 = f\lambda/\pi w_f$ , a result independent of the position of the input waist. Falk<sup>9</sup> has shown that, using a birefringent crystal, the interference pattern in an unfocused beam gives a measure of  $w_0$ , independent of its position.

Except for the measurement of  $w_0$  using the beam size at the focus of a lens or the method of Falk, measurements of the waist size and its position are interrelated. Both can be determined by finding the minimum beam size and its position. This can be a time-consuming procedure, especially with a pulsed system. Alternatively, both can be determined from two measurements made (preferably) simultaneously. The quantities measured are the beam sizes at two different known positions with respect to the back focal point of a lens, one of which can be zero, the other some convenient distance  $D$ . If one of the distances is zero,  $w_0$  and  $z_R$  can be calculated from the measured beam size. Then the position of the input waist can be calculated from the equation

$$y = \frac{f^2 \pm z_R \sqrt{\left(\frac{w'}{w_0}\right)^2 - D^2}}{D}.$$

One of the two values predicted by this equation has to be eliminated. If one cannot be rejected on the basis of its reasonableness, an additional measurement would be required for some other position. Minimum sensitivity conditions obtain for the obvious case of  $D = 0$  and for  $yD = f^2$ . Although the latter value for  $D$  requires a knowledge of  $y$ , some estimate of  $y$  will assist in avoiding this position.

The position of the waist formed by a lens can be determined by observing the size and speed of the speckle pattern produced when the beam is scattered from a moving surface.<sup>10</sup> This is very precise but is restricted to very small waists and gives no quantitative measurement of the waist size. Both position and size can be measured by a scanning technique using a pinhole,<sup>11</sup> wire or slit,<sup>12</sup> or by various schemes involving a knife-edge. Kocher<sup>13</sup> used a chopper wheel and dual photocell to locate a beam waist and measurement aberrations. Mauck<sup>14</sup> discusses knife-edging of beams. Suzuki and Tachibana<sup>15</sup> and Arnaud *et al.*<sup>16</sup> use knife-edge chopper techniques for both waist size and position measurements. Cohen *et al.*<sup>17</sup> use a Ronchi ruling as a multiple knife-edge measurement of the position and size of very small waists. The position of a waist can also be found by finding the position where damage occurs for minimum power or energy. This is most useful for small waists<sup>7</sup> used in machining and trimming applications.

These techniques are most useful for cw or high repetition-rate pulsed systems. For single pulses, Winer<sup>18</sup> used a multiple-lens camera with different neutral density filters on each lens to produce a set of images for measurement. This method depends on being able to make a photographic negative for densitometry. Wiggins *et al.*<sup>19</sup> suggested that a hole grating yields the multiple images required to produce a negative for densitometry. Alternatively, a multiple element photoelectric detector system using storage can be used.

### IV. General Theory for Diffraction in Gaussian Optics

To use interference methods to locate waist positions and sizes, one must develop a general theory for the diffraction of monochromatic single (simplest) transverse mode Gaussian light beams. In this development, we shall identify and describe, for the first time, a phenomenon which we call interorder interference. We shall present a complete theory for not only Fraunhofer but also all types of Fresnel diffraction, under the assumptions of optical elements which are infinite in lateral extent and thin, and propagation angles which are small relative to the optical axis. As a practical matter, we treat the case of transmission diffraction through a series of round holes in an otherwise opaque mask. Accordingly, the entire diffraction amplitude is modulated by the traditional broad, circularly symmetric single-hole diffraction pattern whose width varies inversely with hole radius. Because the grating



size is infinite compared to beam radii, all diffraction maxima are automatically apodized, the diffraction patterns in and of themselves showing no secondary peaks. At the same time these patterns may indeed overlap, at least in their wings, giving rise to unusual interference phenomena often characterized by the presence of closely spaced interference fringes which are most prominent in the regions between the ordinary diffraction pattern maxima.

Interorder interference can be thought of as arising in different ways illustrated simply for the case of a grating comprised of a linear array of holes, having spacing  $d$ , with one hole centered on the beam axis. While the transverse diffraction pattern is solely determined by the slowly varying single-hole diffraction amplitude referred to above, that parallel to the hole array, although modulated by this function, shows more closely spaced peaks arising from the grating. For simplicity, let us now consider the intensity pattern in the region between the zeroth- and first-order diffraction peaks.

(1) Let us envision the different diffractive orders as being comprised of individual beams nominally propagating away from the grating at angles given by  $m\lambda/d$  for the  $m$ th order,  $\lambda$  being the optical wavelength. Because the centers of curvature of the individual beams lie on lines connecting each diffractive beam with the grating but do not coincide with the grating, the centers of curvature for the outgoing  $m$ th order beams are distinct. Consequently, there will be successive regions of constructive and destructive interference between neighboring diffracted beams which are identifiable as interorder interference fringes.

(2) One may envision the zeroth to first interorder interference as arising from the following types of amplitude: that comprised of Huygens wavelets emitted simultaneously at  $t = t_0$  from all holes; and that comprised of Huygens wavelets emitted at  $t = t_0$  from the central hole and at times  $t_n = t_0 - n\lambda/c$  from the other holes,  $n\lambda$  being the retardation path length for any given hole,  $\lambda/c$  being the optical period. Thus, interorder interference can be thought of as a collection of Huygens wavelet interferences for each hole, of waves emitted at different times.

(3) Each of the above pictures appears at first sight to violate one's physical intuition until it is recognized that, indeed, one may envision the incident Gaussian beam as a Fourier superposition of plane waves having a spread in propagation vector components in the direction of the linear array of grating holes. The Fourier components which diffract into the interorder region may indeed do so in different diffractive orders simultaneously, thus at once justifying both of the above descriptions.

(4) Ultimately the method which is most theoretically sound for treating the problem is the explicit summation of the Huygens amplitudes from each hole at any point in the field space, keeping careful account of retardation phases associated with each path, then squaring to obtain the relative intensities.

In the present treatment method 1 is described in detail while method 3 is called on for conceptual insights. Although method 4 ultimately is exact and convenient for numerical evaluation, method 1 has the advantage of yielding an infinite series of terms for the (exact) expression for intensity, with the terms in the series being expressed analytically, often showing rapid convergence. In cases involving slower convergence, it may be more convenient to use method 4 at the outset. In the present work, both methods were carried out for a case of somewhat slow convergence, namely, one in which five grating holes are strongly illuminated. In the range of angles spanned by the zeroth and first diffraction peaks, including interference effects of the  $(-1,0,1,2)$  diffractive orders, the agreement between the results of methods 1 and 4 (the latter of which was considered exact) lay within 3% at all points. The errors which were most severe occurred at the end points of this interval where, respectively, interference with the  $-2$  and  $+3$  orders are expected to contribute more strongly. For the case in which ten holes are strongly illuminated, the relative errors in the  $0-1$  interval, using interference terms corresponding to  $(0,1)$ ,  $(-1,0)$ , and  $(1,2)$ , the relative errors are reduced at all points to within 0.3%.

## V. Fraunhofer Diffraction of Gaussian Beams

Consider a Gaussian beam traveling in the  $+\zeta$  direction with its waist at  $\zeta = 0$ , having an intensity profile

$$I(\zeta, \xi) = \frac{I_0}{\left[1 + \left(\frac{\zeta\lambda}{\pi w_0^2}\right)^2\right]^{1/2}} \exp\left\{-\frac{2\xi^2}{w_0^2 \left[1 + \left(\frac{\zeta\lambda}{\pi w_0^2}\right)^2\right]}\right\} \quad (1)$$

for lateral displacement  $\xi$  in the direction of the linear array of diffracting holes, where we have suppressed the dependence in the direction mutually orthogonal to the  $\xi$  and  $\zeta$  axes for purposes of simplicity. The beam waist is designated by  $w_0$  ( $\gg \lambda$  for small angle approximations) while the beam radius at any distance is

$$w(\zeta) = w_0 \left[1 + \left(\frac{\zeta\lambda}{\pi w_0^2}\right)^2\right]^{1/2}. \quad (2)$$

For any  $\zeta$ , the wave front radius of curvature is

$$R(\zeta) = \zeta \left[1 + \left(\frac{\pi w_0^2}{\zeta\lambda}\right)^2\right], \quad (3)$$

which is consistent with the optical electric field strength

$$E(\zeta, \xi) = \frac{E_0}{\left[1 + i \left(\frac{\zeta\lambda}{\pi w_0^2}\right)\right]^{1/2}} \exp\left[-\frac{\xi^2}{w(\zeta)^2} + i(k\zeta) + \frac{ik\xi^2}{2R(\zeta)}\right]. \quad (4)$$

Let the linear array of holes be inserted into the beam at distance  $\zeta = z$ , with  $z$  being positive for the grating lying on the far side of the beam waist from the light source. One of the holes is centered on the beam axis. To obtain Fraunhofer diffraction, one inserts a positive lens into the beam on the image side of the transmission grating, at any distance whatever from the grating, and

the desired diffraction pattern will then appear on a screen placed at the focal plane of the lens as a function of  $\xi = f\theta$ ,  $f$  being the focal length of the lens, while  $\theta$  is the diffraction angle.

There are several simple concepts which allow one to determine the form of the diffraction pattern at the Fraunhofer plane. The simplest is to note that the grating, when placed in the beam as shown in Fig. 1, does not change the nature of the transmitted beam (i.e., diffracted in zeroth order) aside from lowering its overall intensity. This is clear when it is realized that the incoming beam is simply a Fourier superposition, and each amplitude is transmitted in its own direction, thereby being superposed without change following passage through the grating. The intensity pattern at the Fraunhofer screen, due to the zeroth order by itself is, then, the same as the angular intensity pattern that the original beam would have very far away from its waist,

$$I_0(\theta) = \text{const} \times \exp\left(-\frac{2\pi^2 w_0^2}{\lambda^2} \theta^2\right). \quad (5)$$

Similarly, each  $m$ th order diffraction pattern, by itself, can be seen to be a replica of the zeroth diffracted beam centered on its own central diffraction angle  $\theta_m (= m\lambda/d)$ , thus

$$I_m(\theta) = I_0(\theta - \theta_m), \quad (6)$$

with  $I_0$  given above. It is, in fact, the possible overlap of various order intensities in the Fraunhofer plane which gives rise to the interference. For example, if the grating consists of holes lying much closer together than  $w_0$ , distinctly separated orders are formed with no appreciable interference. This, in effect, corresponds to the traditional use for which diffraction gratings have been employed. [Of course, at distances smaller than the Fraunhofer distances, the orders might not be well separated, with a resulting complexity in the diffraction pattern. If the lens and screen are placed just behind the grating, the interferences are just such as to form a shadow of the grating—just the starting point for inferring far-field diffraction patterns. On the other hand, if the grating spacing is comparable to the beamwidth, we might expect to find single-hole diffraction, leading to an intensity distribution  $\mathcal{F}(\theta)$  in the Fraunhofer plane, or perhaps a two-hole interference pattern. These can each be interpreted as the result of a great many overlapping orders all interfering with one another in each direction  $\theta$  to produce the relatively simple patterns.]

In a more interesting case, the present context, we consider the neighboring orders to be reasonably distinct but not entirely separated, with several grating holes illuminated so that the individual orders by themselves resemble the intensity distribution of the undiffracted beam on a Fraunhofer plane. Hence  $w_0 \approx d \ll w(z)$  which means that one must place the grating several Rayleigh lengths away from the waist position.

Relative to the central angle in each order at distance  $r$  from the central hole in the grating, the wave fronts have identical form prior to intersecting the lens in Fig.

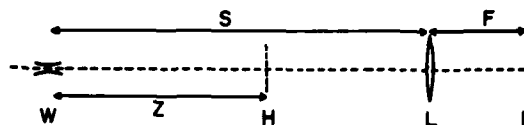


Fig. 1. Schematic of an experimental arrangement. The object waist  $W$  is a distance  $S$  from a lens  $L$  of focal length  $F$  and a distance  $Z$  from a hole grating  $H$ . The Fraunhofer plane  $P$  is one focal length from the lens.

1. Moreover, in Gaussian optics the unique situation exists that the placement of an object waist a distance  $s = f$  from a lens produces an image waist located at distance  $f$  in the image space, that is, in the Fraunhofer plane. Accordingly this situation becomes quite easy to deal with since in all orders the wave fronts, although traveling in different directions, are all planar. The angle at which the  $m$ th beam physically propagates between the lens and the Fraunhofer plane is now clearly  $\theta_m[f - (f - z)]/f$  or  $m\lambda z/fd$ . Accordingly, in the region between the zeroth and first peaks, say,

$$E(\theta) = E_0(\theta) \exp(ik\zeta) + E_1(\theta) \times \exp\left[ik\sqrt{1 - (\lambda z/fd)^2}\zeta + ik\left(\frac{\lambda z}{fd}\right)\xi\right], \quad (7)$$

with  $E_1(\theta)$  similarly given by  $E_0(\theta - \theta_1)$ , so that the intensity is proportional to

$$|E(\theta)|^2 = E_0^2(\theta) + E_0^2(\theta - \theta_1) + 2E_0(\theta)E_0(\theta - \theta_1) \times \cos\left[k\left[\left(\frac{\lambda z}{fd}\right)\xi - \frac{1}{2}\left(\frac{\lambda z}{fd}\right)^2\zeta\right]\right]. \quad (8)$$

In the latter expression,  $\zeta$  represents the optical path difference in the zeroth and first beams as they reach the Fraunhofer plane, which is the same as if both originated at some point on the optical axis formed by the intersection of the first diffraction beam in the space between the lens and the Fraunhofer plane. Thus,  $\xi$  is such that  $\xi = (\lambda z/fd)$  while, of course,  $\theta = \xi/f$ . Hence

$$|E(\theta)|^2 = E_0^2(\theta) + E_0^2(\theta - \theta_1) + 2E_0(\theta)E_0(\theta - \theta_1) \times \cos\left[2\pi\frac{z}{d}\left(\theta - \frac{\theta_1}{2}\right)\right] \quad (9)$$

results showing an interorder interference signal having angular period  $d/z$ .

Now the Fraunhofer diffraction pattern must by definition be independent of the imaging lens separation from the grating, inasmuch as it captures parallel rays for each angle and brings them to the same focal point in the Fraunhofer plane. Let the lens in Fig. 1 be placed at some distance other than the focal distance from the object waist to see in what way one can predict the same diffraction pattern as that given above. The intensity for each  $m$ th order by itself will be unchanged, since this is simply related to the distribution of Fourier components leaving the grating independent of the position of the lens and Fraunhofer planes (which always maintain a separation equal to the lens focal length  $f$ ). The interorder interference structure could differ only if the phase differences at the Fraunhofer plane for the zeroth and first diffraction peaks are changed. Now

the angle at which the  $m$ th diffraction beam approaches the Fraunhofer plane will be given by  $\theta_m[f - (s - z)]/f$  or  $(m\lambda/df)(f + z - s)$ . At the same time, the wave fronts are now curved, because the image waist position is located at a position different from that of the Fraunhofer plane. The curvature of the wave fronts at the focal plane of the lens is known to have the simple form  $R'(f') = -f^2/(s - f)$ . Hence, the phases of the zeroth- and first-order waves which are interfering are  $[k\zeta - 1/2k\xi^2(s - f)/f^2]$  and

$$k \left\{ \left[ 1 - \frac{1}{2} \frac{\lambda}{df} (f - s + z) \right]^2 \zeta + \frac{\lambda(f - s + z)}{df} \xi - \frac{1}{2f^2} \left( \xi - \frac{\lambda f^2}{d} (s - f) \right)^2 \right\}$$

to consistent approximations. Examination of the phase difference, again noting that for the given geometry the effective  $\zeta$  value is such that  $(\lambda/df)(f - s + z)\zeta = \lambda f/d$ , reveals an absence of quadratic terms in  $\xi$  and linear and constant terms equal to those obtained above for the simpler case  $s = f$ . Hence, the Fraunhofer pattern is given independent of  $s$ , as expected.

In the next stage of refinement, it is seen that in principle all orders interfere with one another as indicated for the zeroth and first orders in Eq. (9), although for orders separated by two, the spatial interference signal has twice the spatial frequency and so forth. A complete way in which to represent the diffracted intensity in the  $\xi$  direction for an infinite linear array of holes (with one hole centered on the optical axis) is, therefore,

$$I(\theta) = \mathcal{F}(\theta) \sum_{i,j=-\infty}^{\infty} \sqrt{I_0(\theta - \theta_i)I_0(\theta - \theta_j)} \times \cos \left[ 2\pi \frac{z}{\lambda} (\theta_j - \theta_i) \left( \theta - \frac{1}{2}(\theta_j + \theta_i) \right) \right], \quad (10)$$

$i$  and  $j$  being diffractive order indices, where we have included the slowly varying single-hole diffraction function  $\mathcal{F}(\theta)$ . This expression is exact as long as the small angle approximation holds.

In two dimensions, one can again label all diffractive orders by a single running index  $j$  and assign a set of central angles  $\theta_j$  and intensities to each order determined in accordance with standard diffraction theory through the use of reciprocal lattice vectors for periodic arrays. The general Fraunhofer diffraction intensity function in two dimensions as a function of  $\theta = (\theta_\xi, \theta_\eta)$ ,  $\eta$  being the direction perpendicular to both  $\xi$  and  $\zeta$ , therefore becomes

$$I(\theta) = \mathcal{F}(\theta) \sum_{i,j} \sqrt{I_0(|\theta - \theta_i|)I_0(|\theta - \theta_j|)} \times \cos \left[ 2\pi \frac{z}{\lambda} (\theta_j - \theta_i) \cdot \left( \theta - \frac{1}{2}(\theta_j + \theta_i) \right) \right], \quad (11)$$

the individual order intensity functions having identical functional form. (They could in some cases have different intensities for different types of gratings, however.) From Eq. (11), one sees that each pair of orders gives rise to sets of interference fringes which appear as collections of lines having commensurate periodicities

superposed to give the complete interorder interference pattern. Each set of interorder diffraction lines is, of course, perpendicular to the vector connecting the diffractive orders giving rise to them. Often such superpositions give rise to an appearance of star-shaped maxima as opposed to more circular ones which might arise from products of cosine terms which appear in the above expression. The overall interorder interference pattern appears as a type of moiré pattern.

## VI. Further Considerations

### A. Displaced Gratings

If the 1-D hole grating is displaced along the direction of the array of holes so that no hole coincides with the optical axis, the diffraction pattern suffers some changes. We anticipate these to be periodic, in that if the displacement  $\xi_d$  equals an integral number of  $d$ , the pattern must return to its original form. For  $\xi_d$  less than  $d$ , superposition of Fourier amplitudes again leads us to recognize the zeroth order as remaining unchanged, while the  $m$ th order would be diffracted undisturbed except for a phase advance equal to  $2\pi\xi_d\theta_m/\lambda$  or  $2\pi n(\xi_d/d)$ . Accordingly, the intensity for a 1-D array of holes is modified to the form

$$I(\theta) = \mathcal{F}(\theta) \sum_{i,j} \sqrt{I_0(\theta - \theta_i)I_0(\theta - \theta_j)} \times \cos \left[ 2\pi \frac{z}{\lambda} (\theta_j - \theta_i) \left( \theta - \frac{\theta_j + \theta_i}{2} - \frac{\xi_d}{z} \right) \right]. \quad (12)$$

In two dimensions, the grating could be shifted by a vector displacement  $\xi_d$ , leading to an expression

$$I(\theta) = \mathcal{F}(\theta) \sum_{i,j} \sqrt{I_0(|\theta - \theta_i|)I_0(|\theta - \theta_j|)} \times \cos \left[ 2\pi \frac{z}{\lambda} (\theta_j - \theta_i) \cdot \left( \theta - \frac{\theta_j + \theta_i}{2} - \frac{\xi_d}{z} \right) \right]. \quad (13)$$

Accordingly, as one physically displaces the grating, the interorder interference fringes in the Fraunhofer plane correspondingly are displaced (by one spatial period each time  $\xi_d$  components change by one grating spacing) against a background of fixed diffractive orders.

### B. Negative $z$

If the grating is placed before the object waist and the lens is again placed at an arbitrary location following the grating, with the diffraction image screen again spaced by one focal length from the lens in its image space, the only mathematical difference in the above formulation is that now  $z$  has become negative. Equations (12) and (13) then give the same diffraction patterns as before for  $\xi_d = 0$ , although if  $\xi_d$  is now changed, the interorder interference fringes move counter to their displacement in the positive and equal magnitude case.

### C. Cases Arising from Various Periodicities of the Interorder Interference

Referring to the simplest case, a single line of diffracting holes one of which is centered on the beam axis as described by Eq. (10), it is easily seen that for adja-

cent order interference the number of maxima per order is nominally given by  $z\lambda/d^2$ . If this number is an even integer, there will be a maximum at each neighboring diffraction peak maximum position, which will be complemented by the corresponding interorder interference pattern associated with the peak in question and the nearest neighbor to the other side; similarly, if  $z\lambda/d^2$  has odd integral value, there will be a local interorder interference minimum at these positions, which will be similarly complemented. However, in other situations, a competition exists (which will be complete whenever  $z\lambda/d^2$  is half-integral) by the interorder interferences of the neighboring peaks to either side of each diffractational maxima which tend to suppress the overall interorder interference in the vicinity of these regions. Accordingly, the interorder interference can be variously quite powerful or relatively suppressed in the vicinity of each individual diffractational maximum depending on the actual choice of  $z\lambda/d^2$ .

#### D. Fresnel Diffraction of Gaussian Beams

Consider, as before, a beam having object waist at  $\zeta = 0$ , a 1-D hole grating placed at  $z$ , and a lens placed at a distance  $s > z$ . A screen is placed at the far side of the lens at an arbitrary distance from the lens for purposes of displaying the diffraction pattern. A simple technique which can be used for predicting the Fresnel diffraction at this screen is to imagine the lens to be made up of two lenses,  $L'$  and  $L''$ , as shown in Fig. 2. The focal length of the actual lens  $L$  is denoted by  $f$ , that of  $L'$  and  $L''$  as  $f'$  and  $f''$ , with  $f'' = f'/(f' - f)$ .

The focal length  $f'$  is chosen to be equal to the distance between  $L$  and the screen. Thus the Fresnel diffraction pattern is simply the Fraunhofer pattern associated with the object beam and grating as viewed through the lens  $L''$ . Now it can easily be shown that the beam diameter and wave front curvature of the individual diffractational beams arriving at the screen are those which would have been produced in the absence of  $L''$  by an image beam having a new value for  $w_0$ , called  $w_0''$ , and a new waist position, to which we shall reference a new longitudinal coordinate  $\xi''$ , i.e., the image beam waist is located at  $\xi'' = 0$ . Meanwhile, all diffractational geometric aspects take place as if  $L''$  were removed and the grating were replaced with its standard geometrical image, located at  $\xi'' = z''$  ( $z''$  being the separation, therefore, between the standard geometrical image position of the grating and the Gaussian optical position of the image waist), having apparent hole spacing  $d''$  and hole radius related to the actual values through the standard expression for lateral magnification by the simple lens  $L''$ . In case  $L''$  forms a real image of the grating, these distances become negative. This has no effect on the diffraction pattern formed *per se*; however, if the grating is displaced through distance  $\xi_d$ , the image grating would then be negatively displaced,  $\xi_d'' < 0$ , leading to negative angle displacement of fringes, all things equal. The fact that the image grating may lie to the image side of the lens  $L$ , or perhaps even beyond the screen itself, is interesting but is of no particular physical consequence. An image grating of  $L''$  at  $\pm \infty$

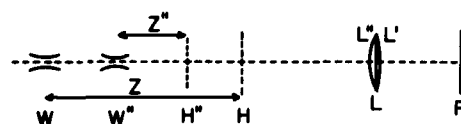


Fig. 2. Schematic for calculation of Fresnel diffraction patterns. Lens  $L$  consists of two parts  $L'$  and  $L''$ .  $P$  is the Fresnel plane for  $L$  and the Fraunhofer plane for  $L'$ . Hole grating  $H$  is a distance  $z$  from the object waist  $W$ .  $W''$  is the image of  $W$  formed by lens  $L'$ , and  $H''$  is the image of the hole grating  $H$  formed by this lens, a distance  $z''$  from  $W''$ .

corresponds to the situation in which the image grating hole diameter and spacings are also infinite, leading to all diffractational orders being superposed, yet still interfering with one another. This, of course, is recognized as the illuminated portion of the grating itself being imaged on the screen. Finally, if there physically is no lens  $L$  between the grating and the screen, one can use the above techniques by choosing a position (separated by an arbitrary distance from the screen) at which we place an imaginary lens combination  $L', L''$ , with  $L'$  having a focal distance  $f'$  equal to the distance of separation with the screen, and  $L''$  having focal length  $f'' = -f'$ . Undoubtedly, the most convenient choice of  $f'$  is the grating-screen separation itself, so that the image grating coincides with the physical grating itself.

The above discussion can be summarized through the mathematical expression for Fresnel diffraction through a periodic 2-D array of holes:

$$I(\theta) = |m'' m_g| \mathcal{F}(m'' \theta) \sum_{ij} \sqrt{I_0(m_g' |\theta - \theta_i'|) I_0(m_g' |\theta - \theta_j'|)} \times \cos \left\{ 2\pi \frac{z''}{\lambda} (\theta_j' - \theta_i') \cdot \left[ \theta - \frac{1}{2}(\theta_j' + \theta_i') - \frac{\xi_d''}{z''} \right] \right\}, \quad (14)$$

with  $m''$  being the standard optical magnification of the grating by  $L''$ ,  $m_g'$  is the corresponding Gaussian image waist magnification by  $L''$ . The diffraction angles  $\theta_n'$  are the actual diffraction angles in the problem (i.e., the angles formed by the beam axis and the line joining the lens at the beam axis with the  $n$ th diffraction spot), related to the corresponding Fraunhofer angles  $\theta_n$  for  $f'' = \infty$  (i.e., no lens  $L''$  necessary) through  $\theta_n' = \theta_n/m''$ . The distance  $z''$  is the displacement (toward the image direction) of the standard geometrical grating image from the Gaussian beam waist image position for lens  $L''$ . Finally,  $\xi_d''$  is the transverse displacement of the standard optical grating image relative to centering on the beam axis, given by  $\xi_d'' = m'' \xi_d$ . One should be aware of the possibility throughout, that  $m''$ ,  $m_g'$ , and  $z''$  or any combination of the three can be variously positive or negative depending on geometry. Finally, while the normalization factor  $|m_g' m''|$  gives a good indication of the intensity behavior due to the magnifications, it may not be entirely accurate, and, if necessary, care should always be taken to assure that the total intensity in the Fresnel pattern matches the energy flux transmitted by the grating.

#### VII. Waist Size and Position Measurements

Two types of experiments were performed using hole gratings made by Buckbee-Mears.<sup>20</sup> The source was

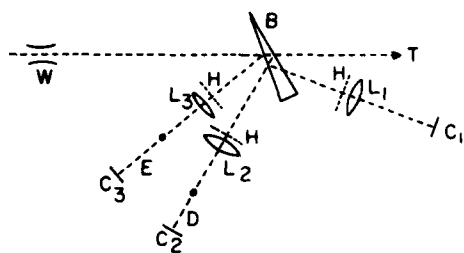


Fig. 3. Schematic of an experimental arrangement to determine the waist size and position. Laser  $W$  is used for damage testing with beam  $T$ . A wedged beam splitter  $B$  sends light through the hole gratings  $H$  to three lenses. Camera backs  $C$  are placed at the focal plane of  $L_1$  and distances  $D$  and  $E$  from the back focal points of  $L_2$  and  $L_3$ .

a Spectra-Physics He-Ne 0.5-mW laser with a nominal beam size of 0.4 mm.<sup>21</sup> Since it has a planohemispherical cavity, the waist is located at the front mirror.<sup>3</sup>

Part of one experiment measured the waist size. The hole radius in the hole grating was 80  $\mu\text{m}$  with a hole spacing of 260  $\mu\text{m}$  in a square array. Scanning a knife-edge at the autocollimated focal point of a 750-cm  $f/12$  mirror, a measure of  $w_0$  could be made with the result of  $369 \pm 6 \mu\text{m}$ . This size was determined using several of the diffracted orders produced by the hole grating,<sup>19</sup> using different positions of the laser source and using different positions of the hole grating in the beam incident on the mirror. In the last case, distances from the mirror of up to 400 cm were used. A chopper was placed near the laser to allow phase-sensitive detection. The distance between the 84.1 and 15.9% transmission points was used as the  $1/e^2$  radius following the theory of Huguley and Loomis.<sup>22</sup>

The second part of this experiment was a mock-up of a pulsed laser damage experiment and is shown schematically in Fig. 3. A wedged beam splitter produced three beams in addition to a direct beam which would be used for testing. The hole gratings placed in front of the lenses were the same as used above. Infrared-sensitive film (Kodak high speed film 2481) developed for 12 min at 20°C in D-76 to yield a contrast index of  $\sim 1$  was used for its sensitivity at the ruby wavelength. Referring to Fig. 3,  $C_1$  is a camera back placed at the focus of  $L_1$  ( $f = 190$  cm) to measure the beam divergence for calculating a value of  $w_0$ .  $C_2$  and  $C_3$  were camera backs placed at selected distances  $D$  and  $E$  from the focal points of lenses  $L_2$  ( $f = 87$  cm) and  $L_3$ . As noted above, the third lens and camera are needed only for selection of the proper root of the equation given. In this case they were not needed since the position of the input waist was known for the He-Ne laser source used. Each film was given an exposure through a step-wedge so that the contrast index for that film could be measured. The transmissions of the negatives  $T(x) = T_0 \exp(\alpha \gamma x^2)$  were fitted to a Gaussian function and its exponent solved for  $\alpha$  using the measured values of  $\gamma$ , the contrast index. The beam size is given by  $\sqrt{2/\alpha}$ . The result was then used to determine the input waist position. The results indicated an input waist of 350  $\mu\text{m}$ , compared with 369  $\mu\text{m}$  measured by the more

precise method above, and a waist position within 4 cm of the output mirror of the laser source. Although the precision of this experiment is not as high as might be expected for other methods that could be used for a continuous source, it demonstrates that the waist size and position can be determined for a single pulse. Data obtained in this way could be used for a study of lensing effects in solid state laser materials or of the effect of amplifiers or frequency doubling.

The second type of experiment uses the theory developed in the previous section to determine the position of the input waist by making measurements of the spacing  $t$  between interference maxima formed by a hole grating. The experimental arrangement is shown schematically in Fig. 1. Using a He-Ne laser placed a distance  $s$  from a lens of focal length  $f$  and placing a hole grating at a distance  $z$  from the waist, it was shown that the separation of interference maxima in the back focal plane of the lens is given by  $t = fd/z$ , where  $d$  is the spacing of the holes in the hole grating. The emphasis was on determining the spacing of the maxima as a function of hole separation and arrangement, the distance of the hole grating from the laser, the distance of the laser from the lens, and different lens focal length.

Figures 4–6 show portions of the interference patterns formed in the focal plane of a mirror of 403-cm focal length. For Fig. 4, a 90° hole grating with holes of radius 110  $\mu\text{m}$  and spacing of 397  $\mu\text{m}$  was located 415 cm from the laser which was  $\sim 800$  cm from the mirror. Using the equation  $z = fd/t$ ,  $z$  was determined to be 390 cm, a result 5% different from the distance actually used assuming the output waist of the laser was at the position of the output mirror. In a more extensive experiment, this hole grating was positioned from 380 to 870 cm from the waist and the resulting fringes photographed. From twenty-three observations the average ratio of the actual value of  $z$  to the computed value was 1.019 with a correlation of 0.990. Other measurements using larger and smaller values of  $z$ , different distances from the laser to the mirror, and different hole gratings showed similar agreement. In general, those for which many fringes were formed yielded smaller errors due probably to the sharpness of the fringes increasing the setability. Since for these cases large  $z$  values are needed, it was established that the error in the position of the waist could be determined to  $\pm 15$  cm. No difference was observed or expected for  $z$  terms of equal size but opposite sign.

Figures 5 and 6 show portions of the patterns formed with other gratings for which  $z$  was chosen so that  $N$ , the number of fringes/order, had particular values. In Fig. 5(A),  $N = 4.0$  for a square grating of  $d = 787 \mu\text{m}$ . In Fig. 5(B),  $N = 3.5$  for the same grating. For Fig. 5(A) the center of the beam was made to coincide with the center of a hole so that constructive interference occurs equally distant between the several orders of diffraction. In Fig. 5(B), the beam was centered between four holes so that an interference minimum occurred between the orders. Figure 6 shows results with two nonsquare gratings. In (A) a grating with spacings of 559 and 970

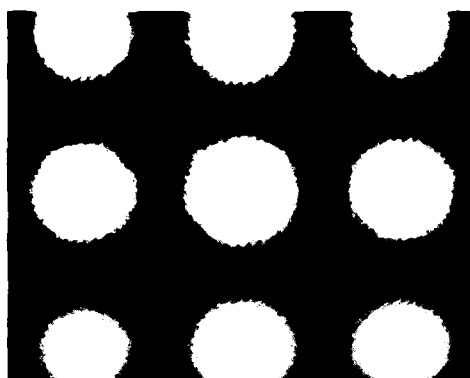


Fig. 4. Central portion of the diffraction pattern formed using a square 90° hole grating with spacing of 398  $\mu\text{m}$  placed 415 cm from a He-Ne laser.

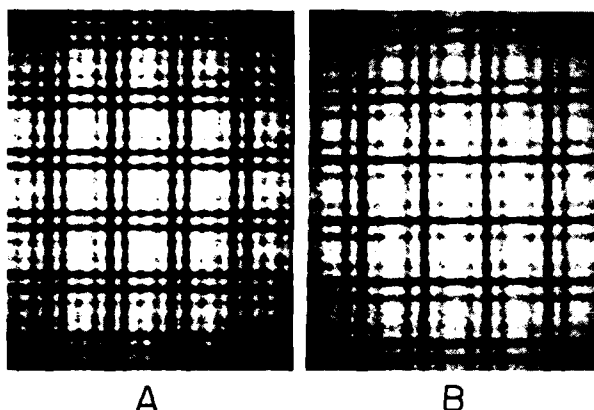


Fig. 5. Central portions of the diffraction patterns formed using a square 90° hole grating with (A) the beam centered on a hole and arranged to produce 4.0 fringes/order, and (B) the beam centered between four holes and arranged to produce 3.5 fringes/order.

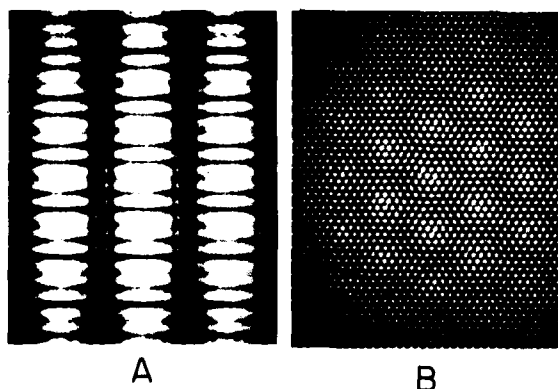


Fig. 6. Central portions of the diffraction patterns formed by nonsquare hole gratings: (A) a grating with spacings of 559 and 970  $\mu\text{m}$ , the beam centered between four holes; (B) a 60° grating arranged to produce 8.0 fringes/order along three directions.

$\mu\text{m}$  in two perpendicular directions was used so that the number of fringes/order was 3 and 9, respectively, with the incident beam centered among four holes. (B) is the result of using a hole grating with 60° hole orienta-

tion at a distance corresponding to 8 fringes/order in three directions.

A study of Eq. (12) shows that, if  $z$ ,  $d$ , and  $\lambda$  were chosen to produce a half-integral number of fringes/order, the intensity at the center  $I(0)$  would show no change due to interference effects between adjacent diffracted orders regardless of the position of the center of the beam with respect to the position of the holes in the hole grating. This suggests an alternative method for the measurement of the waist position. Although the method is not applicable to measurement for a single pulse, it was shown to be the most precise of the methods used in this work. Two types of scanning of the pattern in the Fraunhofer plane were used. First, using an estimate of the correct value of  $z$  needed to produce the half-integral number of fringes/order, the intensity near the center of the pattern is measured, using a slit or pinhole depending on the required geometry, while the hole grating is scanned across the beam. The intensity will change in synchronism with the grating's motion. Changes in the position of the slit will yield a position of smallest intensity change, i.e., at the exact beam center. Then the  $z$  position of the hole grating is changed and the scan by the hole grating repeated. It was found that for a pattern similar to the one shown in Fig. 5(B), a change in  $z$  of 2 cm from the optimum position was detectable. Using the measured value of  $d = 798 \mu\text{m}$ ,  $z$  was calculated to be 352 cm, a result which can be compared with the distance from the hole grating to the front mirror of the laser of 357 cm. It is noted that the intensity variation in principle will not be zero since second-nearest neighbor orders will produce a double frequency variation in intensity which will not reduce to zero.

The importance of these results is that a waist position can be determined independent of the value of  $z_R$  and is therefore most applicable to beams of large  $z_R$  for which many methods of waist position determination are not appropriate.

Support by the Air Force Office of Scientific Research is gratefully acknowledged. A portion of this work has been submitted by J.P. in partial fulfillment of the requirements for the M.S. degree, Dec. 1984.

## References

1. A. G. Fox and T. Li, "Resonant Modes in a Maser Interferometer," *Bell Syst. Tech. J.* **40**, 453 (1961).
2. H. W. Kogelnik and T. Li, "Laser Beams and Resonators," *Appl. Opt.* **5**, 1550 (1966).
3. A. E. Siegman, *Introduction to Lasers and Masers* (McGraw-Hill, New York, 1971).
4. Y. Li and E. Wolf, "Focal Shifts in Diffracted Converging Spherical Waves," *Opt. Commun.* **39**, 211 (1981).
5. W. H. Carter, "Focal Shift and Concept of Effective Fresnel Number for a Gaussian Laser Beam," *Appl. Opt.* **21**, 1989 (1982); G. D. Sucha and W. H. Carter, "Focal Shift for a Gaussian Beam: an Experimental Study," *Appl. Opt.* **23**, 4345 (1984).
6. S. A. Self, "Focusing of Spherical Gaussian Beams," *Appl. Opt.* **22**, 658 (1983).

7. J. T. Luxon, D. E. Parker, and J. Karkheck, "Waist Location and Rayleigh Range for Higher-Order Mode Laser Beams," *Appl. Opt.* **23**, 2088 (1984); J. T. Luxon and D. E. Parker, "Practical Spot Size Definition for Single Higher-Order Rectangular-Mode Laser Beams," *Appl. Opt.* **20**, 1728 (1981); "Higher-Order CO<sub>2</sub> Laser Beam Spot Size and Depth of Focus Determined," *Appl. Opt.* **20**, 1933 (1981).
8. D. Z. Anderson, "Alignment of Resonant Optical Cavities," *Appl. Opt.* **23**, 2944 (1984).
9. J. Falk, "Measurement of Laser Beam Divergence," *Appl. Opt.* **22**, 1131 (1983).
10. J. L. McLaughlin, "Focus-Position Sensing Using Laser Speckle," *Appl. Opt.* **18**, 1042 (1979); H. X. Bai and G. Indebetouw, "Focusing and Aligning of Visual Optical Instruments by Laser Speckle," *Appl. Opt.* **22**, 1609 (1983).
11. P. J. Shayler, "Laser Beam Distribution in the Focal Region," *Appl. Opt.* **17**, 2673 (1978); E. Stijns, "Measuring the Spot Size of a Gaussian Beam with an Oscillating Wave," *IEEE J. Quantum Electron.* **QE-16**, 1298 (1980).
12. R. L. McCally, "Measurement of Gaussian Beam Parameters," *Appl. Opt.* **23**, 2227 (1984).
13. D. G. Kocher, "Automated Foucault Test for Focus Sensing," *Appl. Opt.* **22**, 1887 (1983).
14. M. Mauck, "Knife-Edge Profiling of Q-Switched Nd:YAG Laser Beam and Waist," *Appl. Opt.* **18**, 599 (1979).
15. Y. Suzuki and A. Tachibana, "Measurement of the  $\mu\text{m}$  Sized Radius of Gaussian Laser Beam Using the Scanning Knife-Edge," *Appl. Opt.* **14**, 2809 (1975).
16. J. A. Arnaud, W. M. Hubbard, G. D. Mandeville, D. de la Claviere, E. A. Franke, and J. M. Franke, "Technique for Fast Measurement of Gaussian Laser Beam Parameters," *Appl. Opt.* **10**, 2775 (1971).
17. D. K. Cohen, B. Little, and F. S. Luecke, "Techniques for Measuring 1- $\mu\text{m}$  Diam Gaussian Beams," *Appl. Opt.* **23**, 637 (1984).
18. I. M. Winer, "A Self-Calibrating Technique for Measuring Laser Beam Intensity Distributions," *Appl. Opt.* **5**, 1437 (1966).
19. T. A. Wiggins, T. T. Saito, and R. M. Herman, "Hole Gratings for Laser Damage Testing," *Appl. Opt.* **22**, 3388 (1983).
20. Buckbee-Mears Corp., 245 Sixth Street, St. Paul, Minn. 55101.
21. Spectra-Physics, 1250 W. Middlefield Road, Mountain View, Calif. 94039.
22. C. A. Huguley and J. S. Loomis, "Laser Induced Damage in Optical Materials: 1975," *Natl. Bur. Stand. U.S. Spec. Publ.* **435** (1975), p. 189.

END

DTIC

10-86